Thin-Film Behavior of Poly(methyl methacrylates). 3. Epitaxial Crystallization in Thin Films of Isotactic Poly(methyl methacrylate) Using Crystalline Langmuir–Blodgett Layers

R. H. G. Brinkhuis and A. J. Schouten*

Laboratory of Polymer Chemistry, University of Groningen, Nijenborgh 16, 9747 AG Groningen, The Netherlands

Received October 19, 1991; Revised Manuscript Received January 22, 1992

ABSTRACT: A procedure is introduced using monolayer crystallized films of isotactic poly(methyl methacrylate) (i-PMMA) to induce crystallization in amorphous films of i-PMMA. Use of the Langmuir–Blodgett films as surface crystallization nuclei permits the preparation of highly crystalline films with thicknesses up to the micron regime, not effectively accessible for the conventional technique of building multilayers layer by layer. The orientation of the nucleating overlayers is observed to be copied by the newly crystallized film and extends up to microns from the surface. Anisotropic crystallization of the thin films was observed to result in severe deformations, with a rugged surface relief developing. Even monolayers were shown to be sufficient to induce an oriented epitaxial crystallization; in this respect, local variations in the orientation of the as-deposited monolayers could be visualized by the orientation of the induced crystallization process, permitting some speculations about the original monolayer orientation on the water surface.

Introduction

As has been illustrated by many authors over the past decades, the Langmuir–Blodgett (LB) technique provides a very powerful tool for building well-defined thin films. The thickness regime of these films extends usually up to thicknesses of approximately 1000 Å, although thicker films have been prepared.[1] Some important application areas require films with thicknesses on the order of magnitude of one to several microns. Poly(methyl methacrylate) (PMMA) films in this thickness regime are relevant, e.g., as microlithography resists and as waveguides in optical applications. The conventional Langmuir–Blodgett deposition technique is not very well suited to prepare these kinds of relatively thick films, since the building process would be extremely time consuming. This practical restriction with respect to the film thickness presents a severe limitation of the LB technique in terms of its application potential. In this report, we will discuss an alternative approach, using the Langmuir–Blodgett technique for preparing oriented thin films, extending up to the micron regime, without having to build them monolayer by monolayer.

Langmuir–Blodgett monolayers have been reported to be able to nucleate crystallization of low molecular weight compounds dissolved in the subphase, if the crystal lattices of the monolayer and of the subphase solute match.[2,3] Alternatively, monolayers of long-chain alcohols have been observed to induce ice formation in the water subphase, again by a monolayer-induced nucleation.[4] Following a similar concept, we will discuss our attempts to use transferred Langmuir–Blodgett layers of isotactic poly(methyl methacrylate) (i-PMMA, crystallized in the monolayer according to the process that was extensively discussed in previous publications,[5,6] as *surface crystallization nuclei* for amorphous thin films of i-PMMA, in order to induce a controlled crystallization process in this film. The low spontaneous nucleation density observed in i-PMMA during annealing at the optimal crystallization temperature suggests that it may be possible to cover relatively large distances from the surface using this approach.

Experimental Section

The i-PMMA samples used were highly stereoregular (>97% isotactic triads) and had a narrow molecular weight distribution ($1.1 > D > 1.35$); the lowest molecular weight samples used (less than 5000) were slightly less perfectly isotactic (ca. 90% isotactic triads). Amorphous thin films of i-PMMA on solid substrates were prepared by solution casting (for thicknesses higher than 0.1 μm), or by LB deposition, with subsequent annealing at 180 °C, to ensure that the films were completely amorphous. The substrate materials were either silicon or ZnS (for the IR measurements) or glass (for the microscopy experiments). Polarized infrared transmission experiments were performed according to procedures described in ref 6. The samples were standardly analyzed at positions at least 5 mm from the edges of the substrate and more than 10 mm under the top meniscus line. Microscopy was performed with a Zeiss Axiophot instrument. The atomic force microscope used to probe the surface structure was a home-built IBM instrument, equipped with a fiber-optic interferometer.[7]

Results and Discussion

In two previous publications,[5,6] we extensively discussed the pressure-induced crystallization process that can take place in monolayers of i-PMMA upon compression. During this crystallization process, the expanded amorphous conformation of the i-PMMA chains is exchanged for a crystalline condition, in which the conformation of the i-PMMA presumably is a 10_1 double helix, similar to that proposed for the melt crystal structure. These crystallized monolayers could be transferred from the water surface to solid substrates to build highly oriented crystalline multilayers. Thin films were thus prepared up to thicknesses of up to 1000 Å; preparation of thicker multilayer films is not efficiently possible because of the time-consuming nature of the transfer process, which led us to attempt the procedure as described below.

In Figure 1, the concept of the surface nucleation approach is drawn schematically. Starting with a thin film of amorphous i-PMMA and depositing several monolayers of crystalline i-PMMA on top of it (A), we anticipate that, upon annealing at the crystallization temperature, an *epitaxial* crystallization will result, nucleated by this LB overlayer (B).[8] In order to test whether the surface nucleation idea was feasible, a 300-Å-thick film of i-PMMA,

0024-9297/92/2225-2717$03.00/0

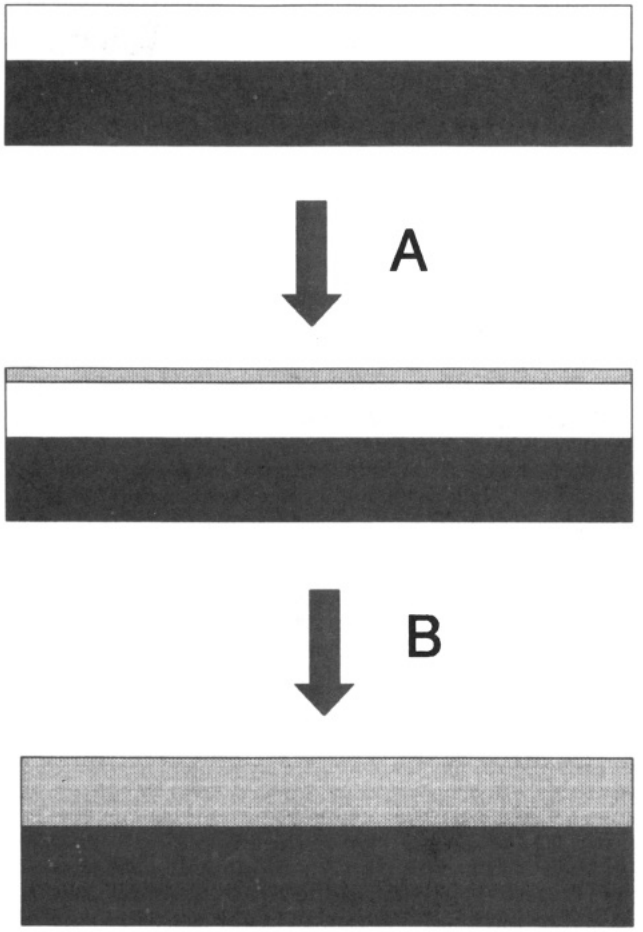

Figure 1. Schematic representation of the surface nucleation concept. An amorphous thin film of i-PMMA is covered by a crystalline LB overlayer (A) and is subsequently crystallized at 120 °C (B).

heated at 180 °C to remove all order present, was covered with an approximately 70-Å overlayer of monolayer-crystallized i-PMMA. Without this crystalline overlayer, a similar 300-Å film did not exhibit any detectable crystallization upon annealing at 120 °C due to the combination of the low spontaneous nucleation density and the extremely low film thickness.[9] With the overlayer present, the film rapidly crystallizes, as illustrated by Figure 2: using favorable molecular weights, crystallization is essentially complete within 15 min. The method of preparation of the amorphous thin film is not important: solution-cast films, spin-coated films, and melted films, originally built by the LB technique, are equally susceptible to the nucleating effect of the crystalline overlayers.

The deposited overlayer is responsible for the nucleation of the crystallization process and thus also controls the *orientation* of the newly crystallized material: since the Langmuir–Blodgett overlayer exhibits a clear preferential orientation, not only parallel to the substrate but also within the XY plane parallel to this substrate (as was extensively discussed in ref 6), the entire film may be expected to adopt these same orientational features upon crystallization. This orientation transfer is actually observed, as is evident in Figure 2: the overlayer used for this experiment was highly oriented with the helix axes parallel to the transfer direction. Similar orientation processes induced by surface layers have also been reported for liquid-crystalline materials.[10,11]

The strategy, described above, clearly allows for a very efficient way to prepare thin films with controlled orientational characteristics, since the orientation of the overlayer can easily be regulated through the proper choice of the molecular weight of the monolayer material and the monolayer crystallization conditions.[6] Langmuir–Blodgett layers of i-PMMA transferred under conditions leading to an orientation of the helices parallel to the dipping direction (as in Figure 2) induce a crystallization with similar orientation characteristics; LB layers transferred with the helix axes oriented perpendicular to the transfer direction[6] can be observed to induce a crystallization process with perpendicular orientational characteristics.

In the rest of this paper, we will refer to monolayers of high molecular weight i-PMMA ($\bar{M}_n$ 770K), crystallized on the water surface by rapid compression, as the nucleating overlayers, unless stated otherwise. These monolayers exhibit a strong orientation of the helices in the transfer direction upon transfer, as was extensively discussed in ref 6. The dipping speed was invariantly 4 mm/min.

Overlayer Thickness. In Figure 3, we have plotted the lateral orientation parameter $L_{C=O}$ (as defined in ref 6) as a function of the overlayer thickness for a substrate thin film of 300-Å amorphous i-PMMA ($\bar{M}_n$ 13K), following annealing at 120 °C for 5 days, with the overlayers deposited according to the specifications given above. We can see that there is a saturation limit at about 50 Å: thicker overlayers do not lead to better orientational characteristics of the resulting structure. In this regime, the $L_{C=O}$ values are similar to those of a multilayer film built completely of transferred LB layers of the same material as used for the overlayer. Lowering the thickness of the overlayer to under 50 Å leads to gradually less perfect orientational characteristics. Still, even for an overlayer corresponding to one monolayer (12 Å), a significant induced orientation is detectable in the crystallized film. The causes for the apparent decrease in the ability of these extremely thin overlayers to impose a lateral orientation will be addressed later.

Thickness of the Amorphous Film. In order to study the depth to which the nucleating and orienting effect can extend into the film, the $L_{\delta(\alpha\text{-}CH_3)}$ is plotted in Figure 4 as a function of the thickness of the amorphous film to be crystallized. The value for $L_{\delta(\alpha\text{-}CH_3)}$ was used instead of $L_{C=O}$ because, for the thickest films, the absorption values for the C=O stretching vibration are too high to be determined accurately. The α-CH_3 symmetric bending vibration at 1388 cm^{-1} exhibits dichroic characteristics qualitatively similar to the C=O stretching vibration. Figure 4 indicates that oriented crystalline thin films can be produced up to thicknesses of 10 μm, although there is a tendency for the crystallization front to slowly lose some of its orientational information upon progressing far into the subfilm, leading to a gradual decrease of the orientation parameter with increasing thicknesses. From microscopy experiments, we learn that competition by spontaneously nucleated spherulitic structures is negligibly small, even for the thickest samples, so that the cause for the loss of orientational information must be the accumulation of defects in the crystallization front upon growth over large distances.

Growth Kinetics. We followed the kinetics of the growth of the crystalline structure into a fairly thick amorphous film (3 μm), nucleated by an oriented overlayer, by alternately annealing the film for 2 h at 120 °C and recording polarized transmission spectra. In Figure 5, the absorption intensity difference of the 1388-cm^{-1} α-CH_3 symmetric bending vibration absorption in the 90° and the 0° spectra is plotted. Only the fraction of the film

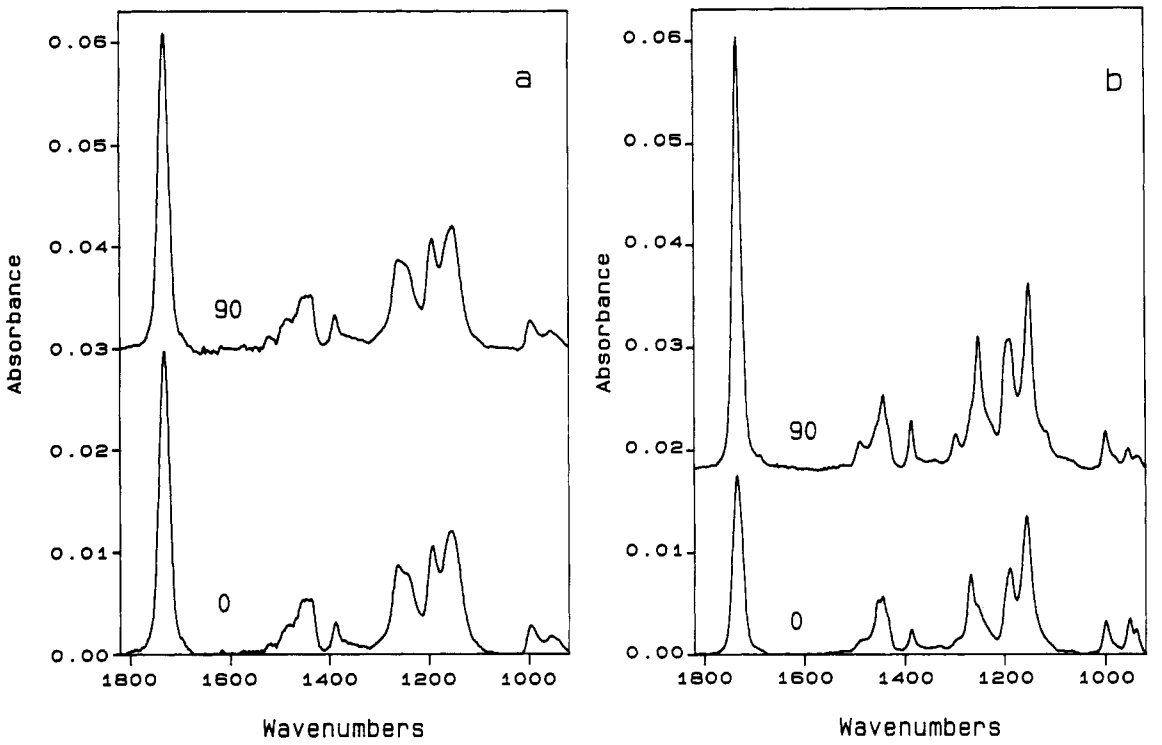

Figure 2. Polarized transmission IR spectra of a 300-Å amorphous thin film of i-PMMA ($\bar{M}_n$ 13K), covered with a 70-Å overlayer of i-PMMA ($\bar{M}_n$ 770K), transferred at 12 mN/m: (a) as deposited; (b) after annealing at 120 °C for 2 h. The polarization direction with respect to the transfer direction is indicated in the figure.

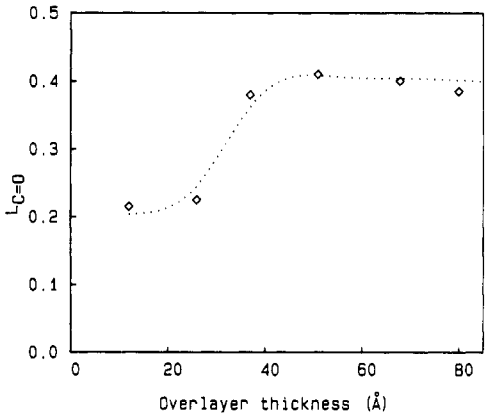

Figure 3. $L_{C=O}$ as a function of overlayer thickness, covering an approximately 300-Å amorphous thin film of i-PMMA ($\bar{M}_n$ 13K), after annealing at 120 °C for 5 days.

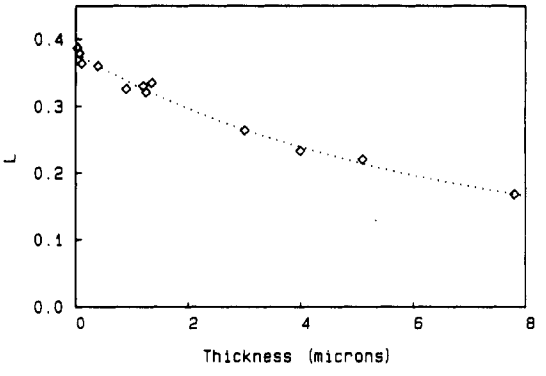

Figure 4. $L_{\delta(\alpha\text{-}CH_3)}$ as a function of the thickness of the amorphous film to be crystallized ($\bar{M}_n$ 13K). Overlayer thickness 70 Å, all samples annealed at 120 °C for 5–8 days.

that has been crystallized will contribute to this difference, since amorphous i-PMMA can be assumed to have isotropic absorption characteristics. An almost straight line from the origin is observed in the beginning of the process, in

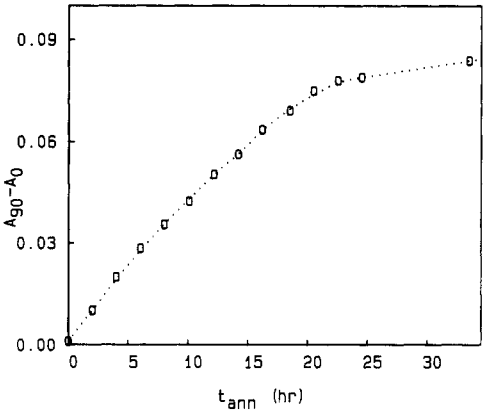

Figure 5. Difference in the absorption intensity of the 1388-cm^{-1} band, between the 90° and 0° polarized transmission spectra, as a function of the annealing time at 120 °C. Matrix film thickness 3 μm, $\bar{M}_n$ 13K. Overlayer thickness 70 Å.

agreement with the picture of a crystallization front progressing through the film, starting from the surface. This characteristic combination of an instantaneous nucleation followed by a one-dimensional growth, corresponding to an Avrami exponent of 1, is similar to that observed for the crystallization in melts of polypropylene at low degrees of undercooling, nucleated by an interfacial region in the film that was oriented by strong shear forces, as reported by Eder et al.[12] In this case, the resulting crystalline layers are characterized by a laminar texture. A similar process was reported by Thomason,[13] describing the growth of transcrystalline boundary layers in fiber-reinforced polypropylene, following a shear-force-associated fiber surface nucleation. The growth rate of the crystallization front can be determined from the time required to reach the saturation zone (approximately 20 h in Figure 5, when the crystallization front has completely traversed the film). This value (1500 Å/h) corresponds very well with the value determined for the linear growth rate of spherulitic structures for this temperature and this

Table I

sample no.	$\bar{M}_w$, $\times 10^{-3}$	r, $\times 10^{-2}$ Å/h
m13	16	15
m8	42	4.0
m7	54	3.5
m5	116	1.3
m4	200	0.5

molecular weight (Table I). The growth mechanism is evidently the same: from the birefringence of the spherulitic structures we can infer that the helices are oriented tangentially with respect to the spherulite, and parallel to the spherulitic growth front, a situation that is also to be expected for the overlayer growth front in the thin films. The melting range of the surface-nucleated films, as observed with a polarization microscope using a hot stage, is identical to that of spontaneously nucleated i-PMMA.

There is a slight tendency for curvature in the 0–20-h region of Figure 5, the curve being slightly less steep at the end of this regime than at the onset of the crystallization process. Careful analysis of difference spectra (between various stages in this initial "linear" regime) indicates that this is not the result of a slowing down of the crystallization rate but rather of a continuous loss of the original orientational characteristics of the newly formed crystalline phase upon progress of the crystallization front, a phenomenon that was also suggested by Figure 4.

Varying the crystallization temperature between 100 and 135 °C does not lead to spectacular variations in the effectiveness of the nucleating and orienting capabilities of the overlayers. The annealing temperature of 120 °C was reported to correspond to the maximal crystallization rate.[14]

Molecular Weight Dependence. Upon variation of the molecular weight of the amorphous film to be crystallized, we can observe that this molecular weight does have an influence on the resulting orientation parameters. In Figure 6, values for $L_{C=O}$, obtained after annealing a 300-Å film with a 70-Å nucleating overlayer for 5 days at 120 °C, are plotted as a function of the molecular weight of the amorphous layer, illustrating this effect. The highest value is obtained for the sample with $\bar{M}_n$ 11 000, with $L_{C=O}$ values even higher than for a film completely built of LB layers of the same type as used for the overlayers. Evidently, the explanation for this fact must be found in a higher level of crystallinity in the low molecular weight material relative to the (postcrystallized) high molecular weight overlayer material. For a more extensive discussion, let us first focus briefly on the characteristics of the normal melt crystallization and the influence of the molecular weight of the i-PMMA. The melt crystallization rate is found to be strongly dependent on the molecular weight: the linear spherulitic growth rate at 120 °C, listed in Table I, falls off rapidly with increasing chain lengths. The variation with molecular weight is stronger than that, e.g., reported by Lemstra for isotactic polystyrene.[15] The DSC melting endotherm for higher molecular weight samples is clearly broadened to the low-temperature side, indicating somewhat less perfect crystallites being formed; in general, a lower (limiting) heat of fusion is found for higher molecular weight fractions. For samples with molecular weights under 12 000, the peak of the endotherm is observed to shift to the low-temperature side, and crystallization is found to be severely suppressed or completely inhibited for molecular weights of less than 5000 for this annealing temperature. This is probably caused by critical chain-length effects: at 120 °C, a minimum length is required for the helical sequences per chain in order to compensate for an

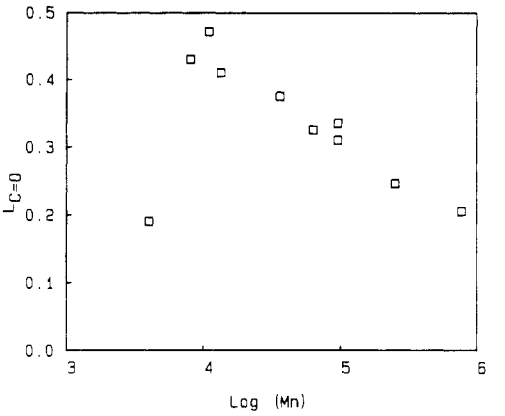

Figure 6. $L_{C=O}$ values for a 300-Å amorphous film of i-PMMA, nucleated by a 70-Å overlayer, annealed at 120 °C, versus the molecular weight of the amorphous film material.

initial entropy loss and to yield thermodynamically stable crystalline structures; for the lowest molecular weight samples, the entropy loss upon crystallization cannot be compensated. A similar suppression of the monolayer crystallization process for these low molecular weight samples was reported in ref 5.

For all molecular weights, the melting endotherm can be observed to change upon annealing: with longer annealing times (even after the film has reached a saturation level of crystallinity) the contribution of material melting at higher temperatures becomes more and more important, an effect that was also reported by other authors.[16,17] Evidently, extensive reorganization processes following the initial crystallization process are responsible for defect elimination or lamellar thickening of the crystallites.

Returning to the overlayer-induced crystallization processes, we observe that, for all molecular weights, the observed crystallization rate is in good agreement with the linear growth rate determined for the spherulitic structures. For all samples, the 5 days allowed for the crystallization should suffice for the crystallization front to traverse the entire film. For higher molecular weights, the resulting crystalline material behind this crystallization front can be expected to have a significantly lower level of crystallinity; this is probably the cause for the lower values observed for the orientation parameter (Figure 6). If we compare the spectrum of a low molecular weight matrix crystallized by one monolayer with that of a high molecular weight matrix crystallized by a thicker overlayer, we can conclude that, in the latter case, the level of crystallinity is lower but that the orientation of the crystalline material itself must be higher (leading to similar $L_{C=O}$ values for both spectra; Figure 7). When the high molecular weight samples are annealed for a long time, after the crystallization front has completely traversed the film, we observe a significant increase in the overall orientation characteristics of the sample with time, due to (slow) reorganization processes in the crystallized matrix (Figure 8).

The fact that the lamellar structures may be less perfect in the case of higher molecular weight samples does not prevent thicker films to be effectively crystallized using the overlayer approach. For films of several microns thickness, similar orientation values can be reached for molecular weights up to 200 000, as for more favorable molecular weights, indicating that the orientation information of the crystallization front is not lost more rapidly. For these higher molecular weights, the process does become very time consuming though. Using very low mo-

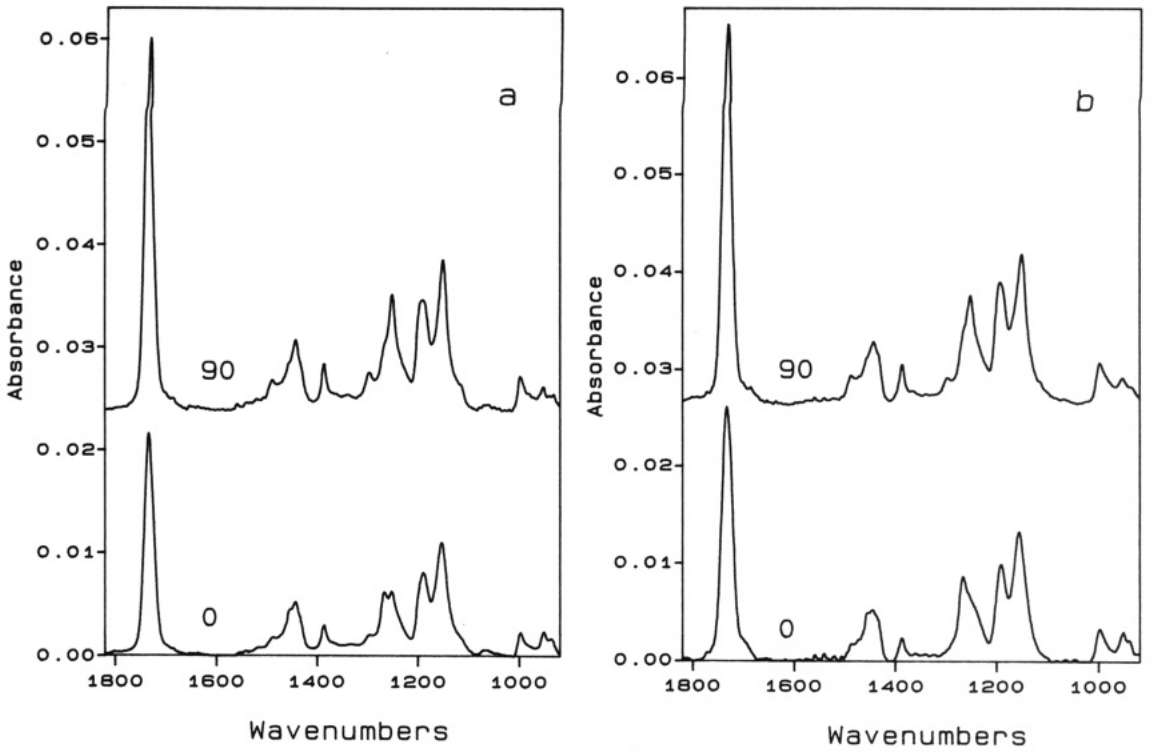

Figure 7. (a) Polarized transmission spectra of an approximately 300-Å amorphous film of i-PMMA ($\bar{M}_n$ 13K), covered with a 12-Å nucleating overlayer, annealed for 5 days at 120 °C. (b) Polarized transmission spectra of an approximately 300-Å amorphous thin film of i-PMMA ($\bar{M}_n$ 770K), covered with a 70-Å nucleating overlayer, annealed for 5 days at 120 °C.

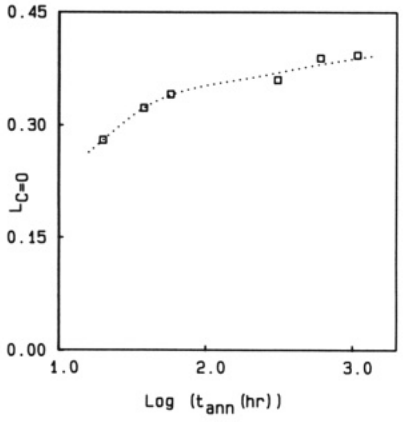

Figure 8. $L_{C=O}$ values for an approximately 600-Å amorphous film of i-PMMA ($\bar{M}_n$ 95K), covered with a 60-Å nucleating overlayer, as a function of annealing time at 120 °C, in the regime after the crystallization front has traversed the film.

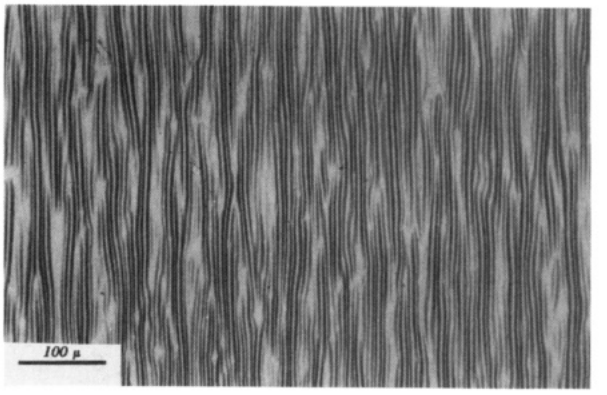

Figure 9. Reflection microscope photograph of an approximately 5-μm-thick film of i-PMMA ($\bar{M}_n$ 13K), crystallized at 120 °C, nucleated by a 60-Å overlayer. Wrinkles are oriented perpendicular to the transfer direction.

lecular weight material ($\bar{M}_n$ 4000) the overlayer approach is not effective (Figure 6) because of the inability of the material to crystalline under these conditions.

Film Morphology. When an amorphous film of i-PMMA, with a thickness in the micron range, is crystallized following nucleation by a highly oriented overlayer, we can observe that the film develops a distinct surface structure. A "buckling" of the film is the result of the highly anisotropic crystallization process. The surface relief is best characterized as a set of wrinkles, with a correlation length of several tens of microns and an orientation always *perpendicular* to the direction of the helices in the crystallized structure. An illustration is given by Figure 9 and10. The development of this surface structure is characteristic for the overlayer crystallized films: the scattering caused by the surface can also be observed in IR experiments, or even with the bare eye. The depth of the surface valleys is on the same order of magnitude as the film thickness, as can be deduced from AFM experiments (Figure 10): a 2-μm roughness was observed for a 4-μm-thick film. Thicker films yield a more rugged surface structure. The wrinkling of the film must be caused by the stresses developing in the top layer of the film due to the anisotropic deformation accompanying the crystallization process; this is also suggested by observations that a "defect" in the film surface (e.g., a dust particle) leads to a high concentration of wrinkles originating from it (Figure 11), due to the concentration of the stress in the film near this defect. This wrinkling effect is somewhat less pronounced when using higher molecular weight samples or lower crystallization temperatures but cannot easily be completely suppressed. Upon melting, the surface structure immediately disappears.

Monolayer Nucleation. In the rest of this paper, we focus on the effect of monolayers as nucleating overlayers. In Figure 3, the orienting effect of monolayers was observed to be less pronounced than that of thicker overlayers. Several explanations can be given for this effect. The thickness of the overlayer associated with a saturation of

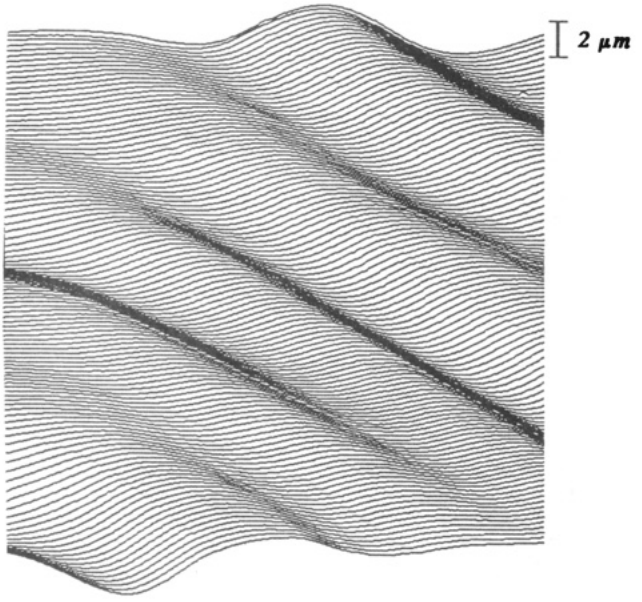

Figure 10. AFM picture of the surface of an approximately 4-μm-thick film of i-PMMA ($\bar{M}_n$ 13K), crystallized at 120 °C, nucleated by a 70-Å overlayer. Wrinkles are oriented perpendicular to the transfer direction.

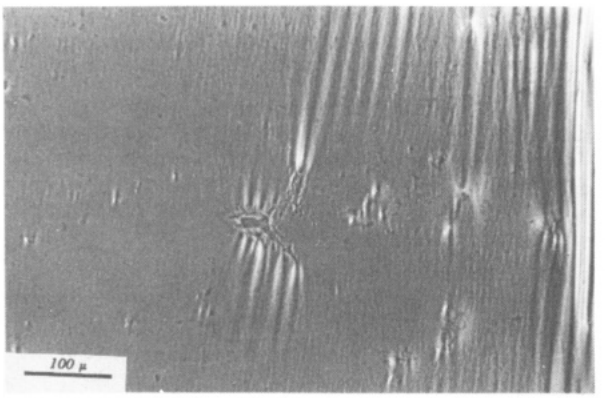

Figure 11. Wrinkles originating from a film defect near the edge of the overlayer-covered area.

the orienting effect is similar to the thickness required for a multilayer on a gold substrate to give a stable crystalline structure: films thinner than approximately 60 Å melt upon annealing at 120 °C.[6] These data should not be directly translated to the monolayers forming the nucleating overlayer, since, in this situation, the LB layers are in contact with a substrate of i-PMMA: the interface energies will be completely different and so may be the stability of a thin crystalline film. Even if a monolayer would not be stable, it is still possible that metastable nuclei grow before melting, enough to acquire dimensions large enough for stability (some time is required for the film to actually reach the crystallization temperature when placed in an annealing oven). If this would be the case, the monolayer would not induce a perfectly continuous crystallization front but instead nucleate the film at random points at the surface, which may lead to a less perfect transfer of the orientation from the monolayer to the film.

Second, in the case of a thicker overlayer film, the structures in this overlayer may first reorganize into a more efficient packing[6] (leading to a better orientation of the helices into a common average direction), prior to inducing crystallization in the amorphous film. In this context, it is useful to note that the first monolayer transferred to the substrate may well have less pronounced

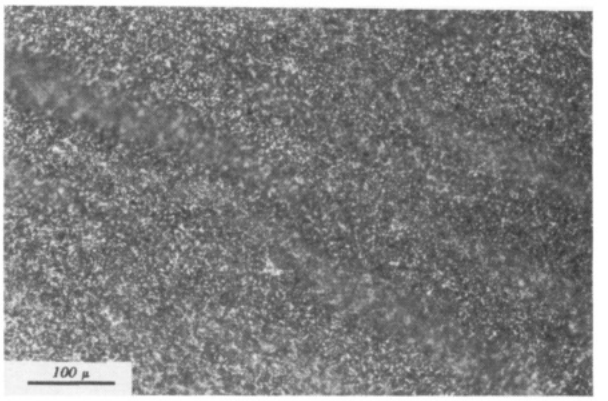

Figure 12. Inhomogeneous orientation observed in a crystalline thin film nucleated by one monolayer. Microscope photograph taken with crossed polarizers.

orientational characteristics compared to subsequent layers, since the orientation must be induced by the flow associated with the transfer process, and this process may not be instantaneously effective (as we will discuss later on). In this case, the layers transferred following the first monolayer may still have a significant effect on the orientation induced in the film, if these layers can also enhance the orientation of the helices in the first monolayer. This scenario may be plausible if the orientation of the various layers is somewhat similar, so that a reorganization into a common crystalline packing is feasible. In an experiment in which a monolayer was transferred, with the helices oriented in the transfer direction, followed by several layers with an orientation perpendicular to that in the first layer, it was observed that the induced orientation was fully determined by the first monolayer: the subsequent layers were not able to invert the orientation of this first layer.

Heterogeneity of the Induced Orientation. The orientation induced in a thick film on a transparent substrate can be easily assessed qualitatively by the birefringence observed using a microscope with crossed polarizers (and also by the local direction of the wrinkle structure of the film). Since the orientation of the crystalline film is directly correlated to the orientation of the monolayer used to induce the crystallization, this provides a unique tool to visualize the *local orientation* of the transferred monolayer, something which would be very hard to study in any other way.

First, we consider the case of the substrate of i-PMMA which was crystallized after one monolayer was deposited during one dipping cycle (during the first downstroke, hardly any transfer is observed). Upon the microscope we see that the orientation induced is *not* homogeneous: close to the meniscus line, there is even a slight preference for the helices perpendicular to the dipping direction, and only the "lower" parts of the film, several millimeters from the top meniscus line, are crystallized with a clear orientation in the transfer direction. In general, and especially in the intermediate region, the film exhibits a domainlike structure (Figure 12), with small domains (several microns in diameter) of varying orientation. The overall orientation is not very clear, and the local orientation in the various domains varies considerably. The domains are obviously too large to be associated with individual monolayer crystallites as transferred from the water surface.[6] The domainlike structure may either indicate a melting of the overlayer film upon annealing, as discussed above, with metastable nuclei inducing the crystallization without being able to form a continuous front, or, alternatively, may reflect an ordering of the an-

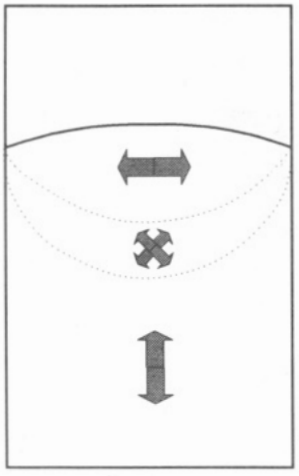

Figure 13. Distribution of the local helix orientation of an as-deposited monolayer, crystallized at the water surface with substrate present across the interface.

isotropic monolayer crystallites in nematically organized domains on the water surface.[18] The observation that, upon using higher crystallization temperatures following the overlayer deposition, the average domain size is somewhat larger than when using lower temperatures appears to argue in favor of the first mechanism. Thin films nucleated by thicker overlayers have a more homogeneous appearance.

For a monolayer deposited after the monolayer was crystallized during compression with the substrate partially *under water* (across the interface, the substrate parallel to the moving barrier, with the amorphous i-PMMA film facing this barrier, the monolayer being transferred during the upstroke movement), we see a different pattern of local orientations: in this case the region close to the meniscus line with a clear orientation perpendicular to the transfer direction is much more pronounced and extends further down the substrate, up to 12 mm from the top meniscus line in the central part of the sample. In Figure 13 the distribution of local orientations of the film (and originally in the as-deposited monolayer) is drawn schematically.

Before the monolayer is transferred, the helical structures evidently possess a preference for an orientation parallel to the substrate located in the monolayer across the air–water interface. This local alignment of the rigid structures in the monolayer may be caused by the direction of the flow caused by the moving barrier upon compression. The substrate acts as a "dam" in the flowing monolayer and thus modifies the flow characteristics of the monolayer,[19] causing the structures to line up parallel to this extra barrier (Figure 14). This original alignment on the water surface is maintained in the beginning of the transfer process: the monolayer flow due to the transfer process itself becomes the dominating factor in later stages and causes an inversal of the preferential orientation direction. The influence of this transfer associated flow may well extend up to some distance into the monolayer on the water surface, leading to some amount of monolayer transfer required for this effect to saturate. Also, the original orientation in the monolayer will be less pronounced with increasing distance from the substrate, the contribution of this effect decreasing after the start of the transfer process. The "new" parallel orientation becomes visible first (i.e., closer to the meniscus line) at the edges of the sample. The reason for this may be 2-fold: in the first place, the original orienting influence of the substrate barrier may be less pronounced near the edges of the

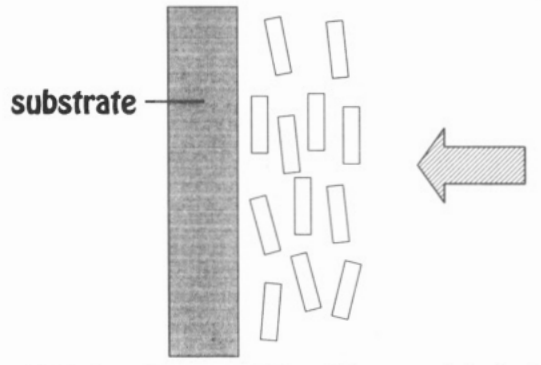

Figure 14. Schematic representation of the suggested orientation in the monolayer at the water surface upon compression with substrate present across the interface, oriented perpendicular to the compression direction (indicated by the arrow).

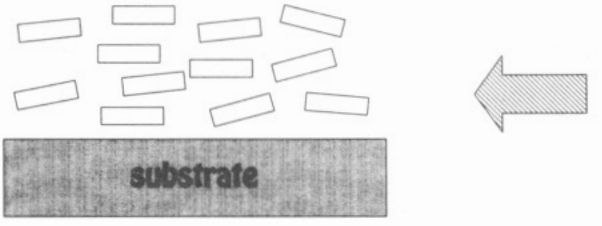

Figure 15. Schematic representation of the orientation process in the monolayer at the air–water interface upon compression with substrate present across the interface, oriented parallel to the compression direction (indicated by the arrow).

substrate, and secondly, the shear forces in the monolayer upon transfer can be expected to be highest near these edges.

If the monolayer is compressed without a substrate acting as an extra barrier, we observe a similar effect, albeit much smaller. In this situation, the fixed measuring barrier may act in a similar manner, its influence extending weakly over the entire trough surface. In accordance with this interpretation, when transferring a monolayer to a substrate, with this substrate oriented perpendicular to the direction of the moving barrier (facing the side of the trough and not present in the interface during the initial compression), we do not observe an initial region in the transferred monolayer with an orientation perpendicular to the transfer direction. An interesting observation is that if we perform the same experiments, but this time not transferring an overlayer from the undisturbed monolayer condition but dipping the substrate in a position where, previous to this experiment, LB layers were transferred to another substrate, the initial region of perpendicular orientation is no longer observable: straight from the start of the deposition process, the monolayer is transferred in a parallel orientation. Apparently, the transfer flow during the previous transfer cycles has left its marks locally in the monolayer. IR experiments also indicate a somewhat better orientation in samples crystallized with these preoriented monolayers.

When the substrate is present in the interface during the monolayer compression, oriented parallel to the direction of flow in the monolayer (Figure 15), and the monolayer is subsequently transferred, we again observe a region under the meniscus line with a perpendicular orientation. Also in this case, the original monolayer orientation on the water surface can be argued to be responsible. When the monolayer flows along the substrate, we are probably dealing with a laminar type flow. Such a flow profile will also cause the rigid structures to align parallel to the substrate wall, eventually leading to

observations similar to the experiment with the substrate parallel to the moving barrier.

Conclusions

The possibility was demonstrated to use Langmuir–Blodgett layers of crystalline i-PMMA as surface-nucleating agents for amorphous thin films of i-PMMA. This method can be used to rapidly produce crystalline thin films, which adopt the orientation of the nucleating overlayers. This method allows for a way to efficiently produce highly oriented films of considerable thicknesses (up to the micron regime) that cannot easily be prepared by the conventional technique of building thin films layer by layer. The idea of inducing oriented crystallization following this approach can be imagined to be also applicable to other systems. Unfortunately, the anisotropic crystallization leads to a strong deformation of the film, with a characteristic surface structure developing, a phenomenon which is of course highly undesirable from the point of view of any possible application. Another disadvantage of this technique is the fact that its practical use is limited to i-PMMA samples with favorable molecular weights, high molecular weights requiring very time-consuming annealing procedures.

The nucleating effect can be used to visualize the local orientation of an as-deposited monolayer. Following this approach, information can be obtained about the original orientation of the helices in the monolayer on the water surface. This original water surface orientation was observed to be clearly affected by the presence of the substrate in the interface during the initial compression.

Acknowledgment. We thank Mr. Kees Grim for recording the AFM scan of the overlayer crystallized thin film.

References and Notes

(1) Tredgold, R. H.; Young, M. C. J.; Hodge, P.; Khoshdel, E. *Thin Solid Films* **1987**, *151*, 441.
(2) Landau, E. M.; Levanon, M.; Leiserowitz, L.; Lahav, M.; Sagiv, J. *Nature* **1985**, *318*, 353.
(3) Mann, S.; Heywood, B. R.; Rajam, S.; Birchall, J. D. *Nature* **1988**, *334*, 692.
(4) Gavish, M.; Popovitz-Biro, R.; Lahav, M.; Leiserowitz, L. *Science* **1990**, *250*, 973.
(5) Brinkhuis, R. H. G.; Schouten, A. J. *Macromolecules* **1991**, *24*, 1487.
(6) Brinkhuis, R. H. G.; Schouten, A. J. *Macromolecules* **1991**, *24*, 1496.
(7) Rudar, D.; Mamin, H. J.; Guenther, P. *Appl. Phys. Lett.* **1989**, *55*, 2588.
(8) The use of the word "epitaxy" is not completely correct, since it strictly refers to a crystallization nucleated by another material; still, since the underlying idea is the same, and because of the lack of an alternative expression to describe the phenomenon, we have chosen to use it throughout this paper.
(9) Billon, N.; Haudin, J. M. *Colloid Polym. Sci.* **1989**, *267*, 1064.
(10) Seki, T.; Tamaki, T.; Suzuki, Y.; Kawanishi, Y.; Ichimura, K.; Aoki, K. *Macromolecules* **1989**, *22*, 3505.
(11) Ito, S.; Kanno, K.; Ohmori, S.; Onogi, Y.; Yamamoto, M. *Macromolecules* **1991**, *24*, 659.
(12) Eder, G.; Janeschitz-Kriegl, H.; Liedauer, S. *Prog. Polym. Sci.* **1990**, *15*, 629.
(13) Thomason, J. L. *Chem. Mag.* **1989**, *44*, 675.
(14) de Boer, A.; Alberda van Ekenstein, G. O. R.; Challa, G. *Polymer* **1975**, *16*, 930.
(15) Lemstra, P. J.; Postma, J.; Challa, G. *Polymer* **1974**, *15*, 757.
(16) Könnecke, K.; Rehage, G. *Makromol. Chem.* **1983**, *184*, 2679.
(17) Lemieux, E.; Prud'homme, R. E. *Polym. Bull.* **1989**, *21*, 621.
(18) Rodriguez, A. L.; Wittmann, H. P.; Binder, K. *Macromolecules* **1990**, *23*, 4327.
(19) Malcolm, B. R. *Thin Solid Films* **1985**, *134*, 201.

Registry No. i-PMMA (homopolymer), 25188-98-1.